Stylasterid corals: A new paleotemperature archive

Ana Samperiz [a,b,*], Laura F. Robinson [a], Joseph A. Stewart [a], Ivo Strawson [a], Melanie J. Leng [c,d], Brad E. Rosenheim [e], Emily R. Ciscato [f], Katharine R. Hendry [a], Nadiezhda Santodomingo [g]

[a] School of Earth Sciences, University of Bristol, Bristol, UK
[b] School of Earth and Ocean Sciences, Cardiff University, Cardiff, UK
[c] National Environmental Isotope Facility, British Geological Survey, Keyworth, UK
[d] School of Biosciences, University of Nottingham, Nottingham, UK
[e] College of Marine Science, University of South Florida, St. Petersburg, USA
[f] Inst. f. Geochemie und Petrologie, ETH Zürich, Zürich, Switzerland
[g] Natural History Museum, London, UK

ARTICLE INFO

ABSTRACT

Stylasterids are a ubiquitous deep-sea coral taxon that build their skeletons from either calcite, aragonite, or both. Yet, robust geochemical proxy data from these corals are limited. In this study, 95 modern stylasterids, spanning a wide range of depths (63 to 2894 m) and ambient seawater temperatures (0 to 17 °C), were tested for their potential use as paleoceanographic archives. Stable oxygen and carbon isotopic composition (δ^{18}O and δ^{13}C) were measured from the main trunk of all specimens and five specimens were further sub-sampled to assess internal chemical variability. The isotope data show non-equilibrium precipitation from seawater for both δ^{18}O and δ^{13}C, with the growing tips of colonies yielding the isotopically lowest values. Overall, the calcitic corals showed lower isotope values for δ^{18}O and δ^{13}C than aragonitic specimens. Within the aragonite corals, we present a δ^{18}O:temperature calibration that exhibits a significant linear relationship with the equation δ^{18}O$_{coral-seawater}$ = $-0.22(\pm0.01) \times T(°C) + 3.33(\pm0.06)$ across a temperature range of 0 to 30 °C, using samples from this study and published data. This work highlights the potential application of stylasterid coral δ^{18}O data to reconstruct paleo seawater temperature.

1. Introduction

Reconstructing the thermal history of the ocean is vital to understanding fundamental aspects of the climate system, including the evolution of ocean heat content (Cheng et al., 2019), past ocean circulation (Marcott et al., 2011), climate sensitivity (Martínez-Botí et al., 2015), and response of marine ecosystems (Hughes et al., 2017). The development of robust paleoceanographic temperature proxies is important to achieve these goals. Pioneering studies in the 1950s first identified the potential use of carbonate fossils as archives for the seawater temperature in which they formed, by finding a temperature dependence of oxygen isotope composition (δ^{18}O) in biogenic carbonates (Emiliani, 1955; Epstein et al., 1953; McCrea, 1950; Urey, 1947). For many years, the δ^{18}O of foraminifera and shallow-water corals have been important

archives of paleotemperatures (Lea, 2014). Although extremely valuable, these archives present inherent limitations to the resolution and geographical extent of the potential reconstructions they provide. In this framework, carbonate-building deep-sea corals are emerging as complementary paleoceanographic archives, as they are unaltered by bioturbation, can be long-lived, and are widely distributed both spatially and bathymetrically (Roberts et al., 2006; Robinson et al., 2014).

Geochemical studies on deep-sea scleractinian and bamboo corals (class Anthozoa) have shown that isotope signatures related to biomineralisation (so-called "vital effects") can mask the temperature dependent fractionation (Emiliani et al., 1978; Heikoop et al., 2000; Smith et al., 2000, 2002; Adkins et al., 2003; Hill et al., 2011). This manipulation of the δ^{18}O and carbon isotope (δ^{13}C) composition of small volumes of seawater taken into the tissue during deep-sea coral biomineralisation makes temperature reconstruction from these taxa challenging. To overcome this limitation, the "lines method" was developed to exploit the linear relationship between stable carbon and oxygen isotope composi-

* Corresponding author at: School of Earth and Ocean Sciences, Cardiff University, Main Building, Park Place, Cardiff CF10 3AT, UK.
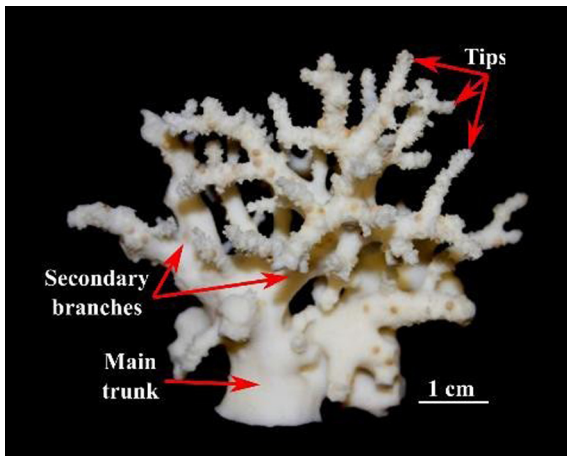*E-mail address:* samperizvizcainoa@cardiff.ac.uk (A. Samperiz).

Fig. 1. Stylasteridae colony (*Inferiolabiata labiata*) from South Orkney (JR15005). Indicated are the different structural parts of the skeleton considered for this study.

tion governed by kinetic isotope fractionation (Smith et al., 2000). In the "lines method," multiple $\delta^{18}O$ and $\delta^{13}C$ analyses are used to determine which part of the skeleton precipitated closest to equilibrium with seawater (Smith et al., 2000). A similar approach was also applied to calcitic bamboo corals (Hill et al., 2011). A variety of other geochemical paleotemperature proxies have been tested in coral carbonates, including clumped isotopes of carbon and oxygen (Ghosh et al., 2006; Thiagarajan et al., 2011; Spooner et al., 2016) and trace metal ratios including Sr/Ca (Beck et al., 1992; Smith et al., 1979) and Li/Mg (Case et al., 2010; Montagna et al., 2014). However, all geochemical approaches applied to date have revealed limitations due to "vital effects" and often location and/or species-specific calibrations are required (Alpert et al., 2016; Fowell et al., 2016; Spooner et al., 2016). Consequently, high-resolution records of intermediate and deep-water temperatures are challenging to obtain and interpret, although their importance over the timescale of human-induced global warming is unequivocal (Gleckler et al., 2016).

There is a pressing need to unlock the potential of other coral taxa and to broaden the scope of ocean temperature proxy development. Stylasteridae (Fig. 1) is a ubiquitous (Fig. 2) and highly diverse family of corals within the class Hydrozoa (Cairns, 2011). Stylasterids are the only known coral taxon with variable mineralogy, calcifying their skeleton out of aragonite or calcite, and occasionally using both $CaCO_3$ polymorphs (Cairns, 2007; Lindner et al., 2008; Cairns, 2011). Despite their diversity and abundance, knowledge about their ecology, physiology and evolution is limited. To date few studies have explored the geochemistry of stylasterid corals and their potential use as paleoceanographic archives. Two studies hinted at a relationship between $\delta^{18}O$ and temperature, with one focusing on the shallow-water genera *Distichopora* and *Stylaster* (Weber and Woodhead, 1972a), and the other on a single specimen (genus *Errina*) from the Azores archipelago (Wisshak et al., 2009). A further study compared taphonomic and diagenetic alteration, as well as $\delta^{18}O$ and $\delta^{13}C$ composition of modern and sub-fossil samples of *Stylaster erubescens* (Black and Andrus, 2012). More recently, ^{14}C measurements in Antarctic stylasterids (genus *Errina*) have been used to trace water mass movements on the centennial time scale (King et al., 2018). Their global distribution across a vast depth range, presence in areas where other archives are rarely found (steep walls and low nutrient waters (Cairns, 1992), as well as their tree-ring like growth bands, raise the potential of these deep-sea corals as high-resolution subsurface ocean archives.

Here, we present the first systematic oxygen isotope calibration of stylasterid corals. We measured $\delta^{18}O$ and $\delta^{13}C$ in modern

samples of seven genera from a wide geographic distribution to test whether this coral taxon can be used as a reliable and useful archive of past subsurface seawater temperature.

2. Methods

2.1. Coral sampling and preparation

Ninety-five stylasterid coral specimens were examined for this study. These were collected during cruises and field campaigns including locations from the Drake Passage (LMG0605; NBP0805; NBP1103), South Orkney Islands (JR15005), Equatorial Atlantic (JC094), North Atlantic (CE14001; JC136; DY081), Galapagos archipelago (AL1508) and Florida Straits (SJ2007) (Fig. 2, Table 1 and Table S1). Species identification of the samples was based on skeletal morphological structures, as described in the literature (Cairns, 1983, 1986a, 1986b, 1991a, 1991b, 2011; Zibrowius and Cairns, 1992), using both optical and scanning electron microscopy (SEM). The 95 modern specimens of stylasterid corals studied included 20 species belonging to seven genera, namely: *Adelopora*, *Cheiloporidion*, *Conopora*, *Errina*, *Errinopsis*, *Inferiolabiata*, and *Stylaster*. Two of the specimens could only be identified to genus level. Corals in this study were collected from depths between 63 m and 2894 m, covering a range of water temperatures from 0 to 10 °C and from 14 to 17 °C.

2.2. Seawater properties

The seawater temperature was estimated for each sample location and depth (Table S2). During cruises NBP0805, NBP1103 and JR15005 CTDs (conductivity-temperature-density) were deployed within 0.5° latitude and longitude from the coral sampling sites. Similarly, during cruises CE14001, JC094, JC136, DY081 and SJ2007 seawater temperature was measured at the sample collection site via an ROV or manned submersible mounted CTD (±5 m depth from collection site). Seawater temperature for samples collected from the Galápagos archipelago during cruise AL1508 was extracted from the GLODAP v2 bottle data database (Lauvset et al., 2016) (<0.2° latitude and ∼5° longitude difference). All cruise-derived CTD temperatures were compared to the closest available data in GLODAP v2 (Table S2). The degree of agreement between data sources was variable (mean difference = ±0.3 °C), with 75% of the data showing a difference of <±0.4 °C. Hence, we take ±0.4 °C to be the estimated uncertainty on coral growth temperatures. All figures and tables in this manuscript report the temperature measured on site by the co-located CTD, where available.

The seawater $\delta^{18}O$ and dissolved inorganic carbonate $\delta^{13}C$ ($\delta^{13}C_{DIC}$) were also obtained for each sample location (Table S1). Seawater samples were collected via Niskin bottles during cruises NBP0805, NBP1103 and DY081 (attached to the rosette), and JC094 (attached to the ROV) and measured for $\delta^{18}O$ and $\delta^{13}C$ back in the laboratory (Hendry et al., 2019; Spooner et al., 2016).

For samples collected during cruises JR15005, CE4011, AL1508, JC136 and SJ2007 additional seawater oxygen and carbon isotopic compositions were obtained from the Global Seawater Oxygen-18 Database v1.22 (Schmidt et al., 1999).

2.3. Coral mineralogy

The mineralogy of 56 corals, from the 95 selected for this study, was determined by X-ray diffraction (XRD). The subset of 56 corals was selected to include all the specimens of genera known to biomineralise their skeletons of either aragonite or calcite (or both). These included *Cheiloporidion sp.* (all 8 specimens of this study), *Conopora sp.* (6 out of 15 specimens), *Errina spp.* (7 out of
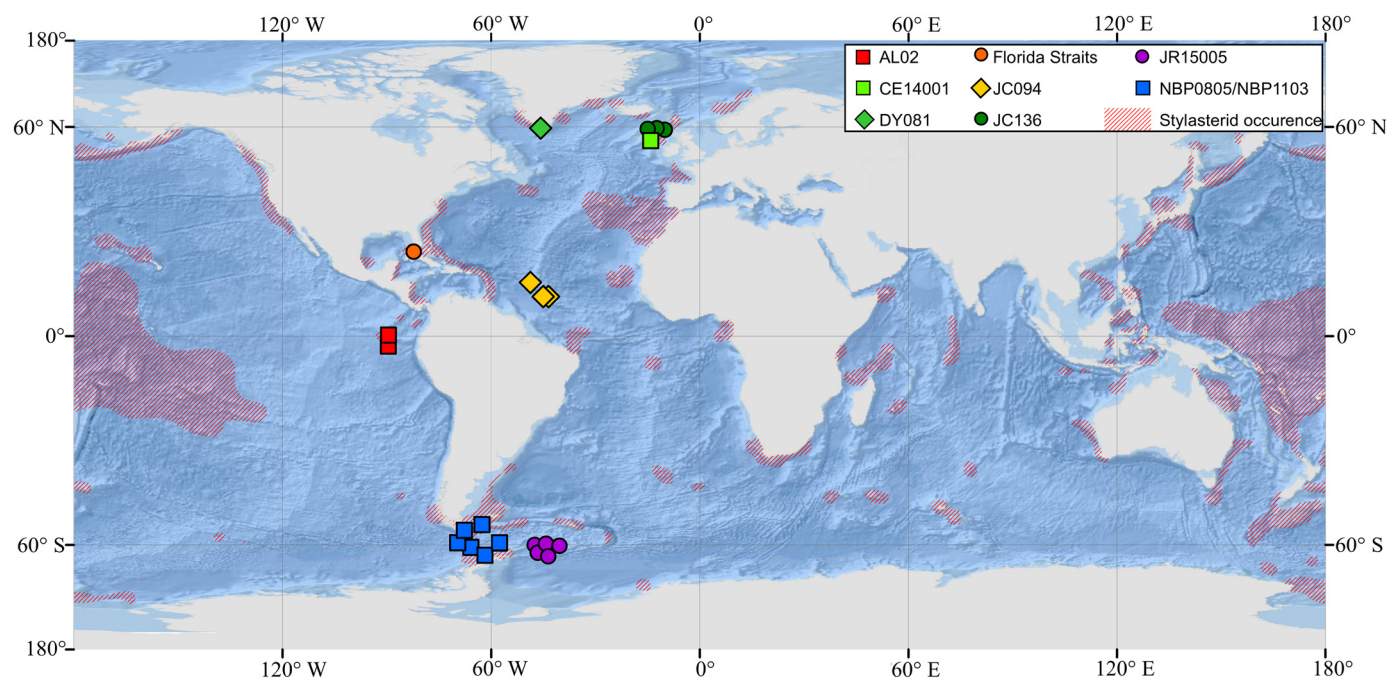
Fig. 2. Distribution of stylasterid corals. Red cross-hatching represents published stylasterid distributions modified from Cairns (1992). Symbols show the locations of the samples of this study collected during 10 field expeditions. (For interpretation of the colours in the figure(s), the reader is referred to the web version of this article.)

10 specimens), *Errinopsis sp.* (all 12 specimens), *Inferiolabiata spp.* (8 out of 17 specimens) and *Stylaster spp.* (15 out of 27 specimens).

The selected specimens were subsampled perpendicular to the vertical growth axis across the main skeletal branch or central trunk of the colony, using a dental drill. Subsamples of ∼0.5 g were powdered using an agate pestle and mortar. Samples were analysed by X-Ray diffraction (XRD) at the University of Manchester using a Bruker D8Advance diffractometer, with a wavelength (λ) of 1.54060 Å and 2θ ranging from 5 to 70 (Davis et al., 1986; Dickinson and McGrath, 2001). This quantitative technique identifies skeletal mineralogy as well as the relative proportions of each polymorph.

2.4. Stable isotope composition of the coral skeleton

All 95 coral specimens were analysed for their $\delta^{18}O$ and $\delta^{13}C$ by taking subsamples from the surface of the central trunk of the coral colony, thus sampling modern skeletal material, deposited shortly before sample collection (Fig. 1). Surface aliquots were prepared using a scalpel to scrape off ∼0.1 mg from the surface layer of the coral skeleton into a fine powder. For specimens for which only a portion of the colony was collected, the largest available branch was sampled. An additional, twenty-two specimens were analysed for bulk $\delta^{18}O$ and $\delta^{13}C$, thus subsampling skeletal material deposited during the entire lifespan of the specimen. Bulk aliquots were prepared with a dental drill, cutting a section perpendicular to the vertical growth axis across the central trunk of the colony. Samples were further powdered using an agate mortar and pestle.

To evaluate $\delta^{18}O$ and $\delta^{13}C$ variation within a single skeleton, five specimens (one calcitic, *Cheiloporidion pulvinatum*, and four aragonitic, *Errina antarctica, Inferiolabiata labiata, Inferiolabiata lowei,* and *Stylaster densicaulis*) were also sampled at the tip of a distal branch and three of these (*Cheiloporidion pulvinatum, Errina antarctica* and *Stylaster densicaulis*) also in a secondary branch. Intra-specimen $\delta^{18}O$ and $\delta^{13}C$ variability within the same visible growth band of a single colony was also examined in an aragonitic specimen of *Errina antarctica*. Eight subsamples were ob-

tained from the same growth band at intervals of 5 mm along a branch, parallel to the vertical growth axis. In this specimen $\delta^{18}O$ and $\delta^{13}C$ were also measured in a cross-section of a secondary branch, with one sample from each growth band. A total of 13 subsamples were obtained at intervals of ∼0.5 mm (the width of each growth ring) on a cross-section, perpendicular to the vertical growth axis.

Coral skeleton $\delta^{18}O$ and $\delta^{13}C$ were analysed at the British Geological Survey using an IsoPrime dual inlet mass spectrometer connected to an attached Multiprep device. The aliquots of coral samples and standards were loaded into glass vials that were evacuated before addition of anhydrous phosphoric acid (H_3PO_4) at 90 °C. The carbon dioxide (CO_2) obtained from the digestion of coral $CaCO_3$ was collected for 15 min, cryogenically purified, and transferred to the mass spectrometer. $\delta^{13}C$ and $\delta^{18}O$ values were calculated using an in-house laboratory calcite standard calibrated against NBS-19. To obtain the $\delta^{18}O$ and $\delta^{13}C$ of aragonitic samples, an aragonite-acid fractionation factor of 1.00855 was applied to the gas values. The Craig correction was applied to account for $\delta^{17}O$ (Craig, 1957). The analytical reproducibility of the standard calcite in each measurement session was <0.04‰ for $\delta^{18}O$ and <0.07 for $\delta^{13}C$.

All coral $\delta^{18}O$ and $\delta^{13}C$, and $\delta^{13}C_{DIC}$ data are reported as per mil (‰) relative to the Vienna Pee Dee Belemnite (VPDB) standard. Seawater values of $\delta^{18}O$ are reported as per mil (‰) relative to Vienna Standard Mean Ocean Water (VSMOW).

3. Results

3.1. Coral skeletal mineralogy

Of the 56 specimens analysed for skeletal mineralogy, 16 were calcitic (>93% calcite) and 40 were aragonitic (>93% aragonite) (Table S1). The 39 samples that were not analysed for their mineralogy were assumed to be aragonitic based on prior observations that they belong to genera that always present aragonitic skeletons (Cairns and Macintyre, 1992).

Table 1
Number of specimens of each genus collected at the locations, depth range at which they were collected and seawater temperature at said depths.

Cruise	Sampling location	Lat (°N)	Lon (°W)	No of samples	Genera	Sample depth range (m)	Temp. (°C)
JR15005 (South Orkney Islands)	Area 2a	−62.16	−44.98	1	*Conopora sp.*	726	0.3
				3	*Inferiolabiata sp.*	518-734	0.2
				1	*Stylaster sp.*	726	0.3
	Area 2b	−62.33	−44.54	1	*Conopora sp.*	1629	0.1
				1	*Errina sp.*	1000	0.2
	Area 3	−62.32	−46.77	4	*Conopora sp.*	469-775	0.1-0.3
				2	*Inferiolabiata sp*	773-775	0.3
	Area 4	−60.35	−46.68	2	*Conopora sp.*	529-835	0.3-0.4
				1	*Inferiolabiata sp.*	1403	0.1
	Area 5	−60.49	−44.52	1	*Conopora sp.*	598	1.0
				2	*Errina sp.*	362-522	0.7
				2	*Inferiolabiata sp.*	522-598	0.7-0.9
				3	*Stylaster sp.*	522-632	0.7
	Area 6	−60.57	−41.05	2	*Inferiolabiata sp.*	239-651	0.6-0.9
				1	*Stylaster sp.*	651	0.7
NBP0805/ NBP1103/ LMG0605 (Drake Passage)	Antarctic Peninsula	−63.07	−61.65	1	*Stylaster sp.*	576	1.8
	Burdwood Bank	−54.72	−62.24	4	*Cheiloporidion sp.*	316-715	3.9-4.5
				3	*Errina sp.*	130-312	4.5-5.8
				2	*Inferiolabiata sp.*	715	3.9
				1	*Stylaster sp.*	715	3.9
	Cape Horn	−57.00	−67.58	1	*Cheiloporidion sp.*	942	3.5
				2	*Conopora sp.*	1049	3.2
				1	*Inferiolabiata sp.*	942	3.5
				3	*Stylaster sp.*	741-1012	3.2-4
	Interim Seamount	−60.69	−66.06	1	*Cheiloporidion sp.*	1545	1.6
				1	*Inferiolabiata sp.*	794	2.1
				1	*Stylaster sp.*	982	2.0
	Sars Seamount	−59.73	−68.87	1	*Adelopora sp.*	656	2.7
				2	*Cheiloporidion sp.*	692-900	2.1-2.2
				2	*Errina sp.*	798	2.4
				12	*Errinopsis sp.*	1654	2.0
				3	*Inferiolabiata sp.*	656-869	2.7-2.5
	Shackleton Fracture Zone	−60.18	−57.85	2	*Conopora sp.*	770-999	1.9-1.8
				1	*Errina sp.*	770	2.0
				5	*Stylaster sp.*	770-1272	1.7-1.9
JC094 (Equatorial Atlantic)	Vayda Seamount	14.51	−48.14	1	*Conopora sp.*	1971	3.4
				1	*Errina sp.*	826	6.1
	Vema Fracture Zone	10.44	−44.34	3	*Adelopora sp.*	568-727	6.2-7.3
				1	*Conopora sp.*	2894	2.3
JC136 (North Atlantic)	George Bligh Bank	58.71	−13.83	1	*Stylaster sp.*	909	7.2
	Rockall Bank	58.38	−13.55	2	*Stylaster sp.*	820	7.6
	Rosemary Bank	59.10	−10.66	2	*Stylaster sp.*	845	8.2
CE14001 (North Atlantic)	Rockall Bank	56.67	−13.90	1	*Stylaster sp.*	516	9.2
DY081 (North Atlantic)	Cape Farewell	59.92	−46.50	1	*Stylaster sp.*	939	5.9
Florida Straits	Pourtalès Terrace	24.33	−81.68	2	*Stylaster sp.*	192	15.0
AL02 (Galápagos)	NW Floreana	−1.24	−90.56	1	*Stylaster sp.*	176	15.0
	SE Santiago	0.38	−90.44	1	*Stylaster sp.*	63	17.3

3.2. Isotope variability

Values of δ^{18}O and δ^{13}C from the main trunk of aragonitic stylasterid corals ranged from −0.40 to +3.43‰ and from −3.05 to +2.30‰, respectively. Data from calcitic stylasterids exhibited a range of +0.40 to +1.68‰ for δ^{18}O and of −6.63 to +0.19‰ for δ^{13}C, respectively (Fig. 3a). Bulk measurement of δ^{18}O and δ^{13}C of aragonitic specimens ranged from +0.03 to +3.32‰ and from −2.68 to +1.73‰. Bulk data from calcitic specimens was of +1.73‰ and +1.78‰ for δ^{18}O, and −4.62‰ and −4.67‰ for δ^{13}C (Fig. 3a). Linear relationships are observed for the δ^{13}C:δ^{18}O data of the main trunk samples. Least squares regression analyses yielded a slope of 1.66 and R^2 value of 0.36 (p-value $<$ 0.001). Classifying datasets by genus yield slopes from −0.65 to 4.29, and R^2 values from −0.99 to 0.78 (Table 2).

In the five specimens with repeat analyses, the tips were ~1‰ and ~3‰ lower in δ^{18}O and δ^{13}C respectively than main trunk and secondary branches (Fig. 4). The positive slopes for the δ^{13}C:δ^{18}O relationships within each coral show no clear difference between the calcitic and aragonitic specimens. ANOVA tests ($\alpha = 0.05$) demonstrate that fractionation levels of growing tips are statistically different to the main trunk and secondary branches (p-value $<$ 0.001).

The isotopic composition of samples from within a single growth band of *Errina antarctica* yielded a δ^{18}O range from +1.14 to +1.45‰ and a δ^{13}C range from −1.51 to +1.50‰. The isotopic composition across the growth bands of the trunk yielded a δ^{18}O range from +0.80 to +1.46‰, and a δ^{13}C range from −1.50 to −0.59‰. The sample from the centre of the trunk yielded the lowest δ^{18}O and δ^{13}C (Fig. 5). Least squares linear regression of
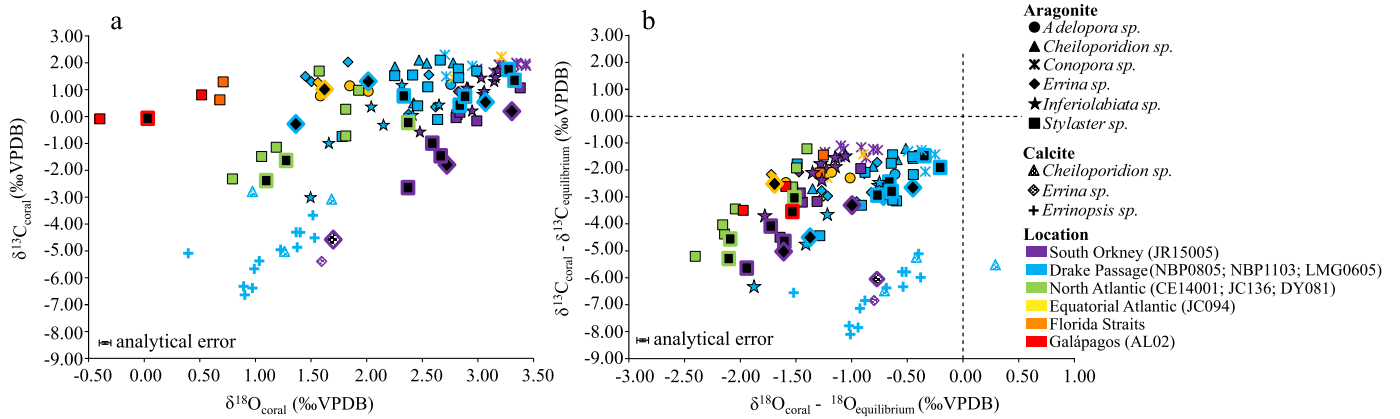
Fig. 3. Stylasterid coral δ^{13}C v. δ^{18}O. (a) Coral δ^{13}C vs. δ^{18}O and (b) Coral δ^{13}C vs. δ^{18}O offsets from estimated equilibrium values for main trunk samples from the 95 specimens of this study. Colour-filled symbols are main trunk samples, black-filled symbols outlined in colour are bulk samples. Colour codes indicate location were the specimen was collected. Dashed black lines represent isotopic equilibrium for oxygen and carbon isotopes.

Table 2

Regression data for all 95 main trunk samples, classified by area collected, by genus and by mineralogy. R^2 represents the linear correlation between δ^{13}C and δ^{18}O. "Vital effects" during mineralisation result in the discrimination against the heavy isotopes of both carbon and oxygen resulting in strong linear correlation.

Dataset grouped by		Mineralogy	n	δ^{13}C:δ^{18}O			
				Intercept	Slope	R^2	p-value
Location	South Orkney	All	36	−11.63	4.1	0.92	<0.001
		Aragonite	33	−10.72	3.8	0.8	<0.001
		Calcite	3	−12.19	4.29	0.8	>0.1
	Drake Passage	All	57	−7.27	3.15	0.68	<0.001
		Aragonite	42	−1.41	0.95	0.18	<0.01
		Calcite	15	−7.01	1.84	0.23	<0.1
	N. Atlantic	All (Aragonite)	10	−3.59	1.94	0.41	<0.1
	Eq. Atlantic	All (Aragonite)	7	−0.1	0.64	0.7	<0.1
	Florida Straits	All (Aragonite)	2	−14.53	22.24	–	–
	Galápagos Islands	All (Aragonite)	3	0.16	0.99	0.53	>0.1
Genus	*Adelopora sp.*	All (Aragonite)	4	0.42	0.29	0.31	>0.1
	Cheiloporidion sp.	All	8	−8.35	3.93	0.78	<0.01
		Aragonite	5	−0.64	0.93	−0.24	>0.1
		Calcite	3	−3.58	−0.03	−0.99	>0.1
	Conopora sp.	All (Aragonite)	15	1.19	0.22	−0.02	>0.1
	Errina sp.	All	20	−1.63	0.6	−0.03	>0.1
		Aragonite	17	1.93	−0.65	0.09	>0.1
		Calcite	3	−12.19	4.29	0.8	>0.1
	Errinopsis sp.	Calcite	12	−7.24	1.82	0.36	<0.1
	Inferiolabiata sp.	All (Aragonite)	17	−4.45	1.85	0.69	<0.001
	Stylaster sp.	All (Aragonite)	39	−0.73	0.43	0.07	<0.1
All		All	115	−3.9	1.66	0.36	<0.001
		Aragonite	97	−0.91	0.64	0.17	<0.001
		Calcite	18	−6.46	1.27	0.15	<0.1

data from the same growing band yielded a δ^{18}O and δ^{13}C relationship with a slope of 4.77 ($R^2 = 0.51$, p-value < 0.1), and the least squares linear regression analysis from the cross-section samples yielded a relationship with a slope of 3.24 ($R^2 = 0.73$, p-value < 0.001). The linear regression yielded by the surface samples of the main trunk, secondary branches and tip calculated previously had a slope of 2.75 ($R^2 = 0.87$, p-value < 0.001).

3.3. Isotope fractionation

To test if stylasterid corals precipitate their skeleton in isotope equilibrium, we compared measured δ^{18}O and δ^{13}C values to cal-culated equilibrium values from each sample location. For δ^{18}O, aragonite isotope equilibrium was calculated using the aragonite-H_2O fractionation factor from Grossman and Ku (1986). Calcite equilibrium was calculated using the calcite-H_2O fractionation factor from O'Neil et al. (1969). Equilibrium values for δ^{13}C were estimated using fractionation factors from Romanek et al. (1992). The estimated equilibrium values were subtracted from the coral isotopic value (δ^{18}O (δ^{13}C)$_{coral}$ − δ^{18}O(δ^{13}C)$_{equilibrium}$) to obtain the fractionation values for each sample (Fig. 3b).

Fractionation values from isotopic equilibrium of aragonitic colonies ranged from −2.41 to −0.16‰ for δ^{18}O and from −6.37 to −1.05‰ for δ^{13}C. Calcitic colonies ranged from −1.52 to

Table 3

Offset range and mean offset values (and SD) from $\delta^{18}O$ and $\delta^{13}C$ equilibrium of main trunk samples. Analytical error is ±0.07 for $\delta^{13}C$ and ±0.04 for $\delta^{18}O$. Analyses were made classifying specimens by mineralogy and by genera.

Species	n	$\delta^{18}O$ offset ($\delta^{18}O_{equilibrium} - \delta^{18}O_{coral}$)				$\delta^{13}C$ offset ($\delta^{13}C_{equilibrium} - \delta^{13}C_{coral}$)			
		Min (‰)	Max (‰)	Mean (‰)	SD (σ)	Min (‰)	Max (‰)	Mean (‰)	SD (σ)
Aragonitic corals	97	−2.41	−0.16	−1.16	0.5	−6.37	−1.05	−2.6	1.38
Calcitic corals	18	−1.52	0.28	−0.69	0.4	−8.09	−5.13	−6.48	0.87
Adelopora sp. (Aragonite)	4	−1.6	−0.62	−1.11	0.4	−2.43	−2.05	−2.21	0.17
Cheiloporidion sp. (Aragonite)	5	−1.36	−0.46	−0.75	0.36	−2.66	−1.16	−1.75	0.56
Cheiloporidion sp. (Calcite)	3	−0.71	0.28	−0.28	0.51	−6.47	−5.22	−5.73	0.66
Conopora sp. (Aragonite)	15	−1.25	−0.26	−0.82	0.33	−2.25	−1.04	−1.37	0.35
Errina sp. (Aragonite)	17	−2.03	−0.39	−1.2	0.34	−4.74	−1.68	−2.98	0.87
Errina sp. (Calcite)	1	na	na	−0.8	–	−6.84	−6.07	−6.34	0.43
Errinopsis sp. (Calcite)	12	−1.52	−0.39	−0.79	0.33	−8.09	−5.14	−6.63	0.93
Inferiolabiata sp. (Aragonite)	17	−1.88	−0.75	−1.22	0.3	−6.37	−1.44	−2.84	1.27
Stylaster sp. (Aragonite)	39	−2.41	−0.16	−1.27	0.61	−5.66	−1.17	−2.96	1.22

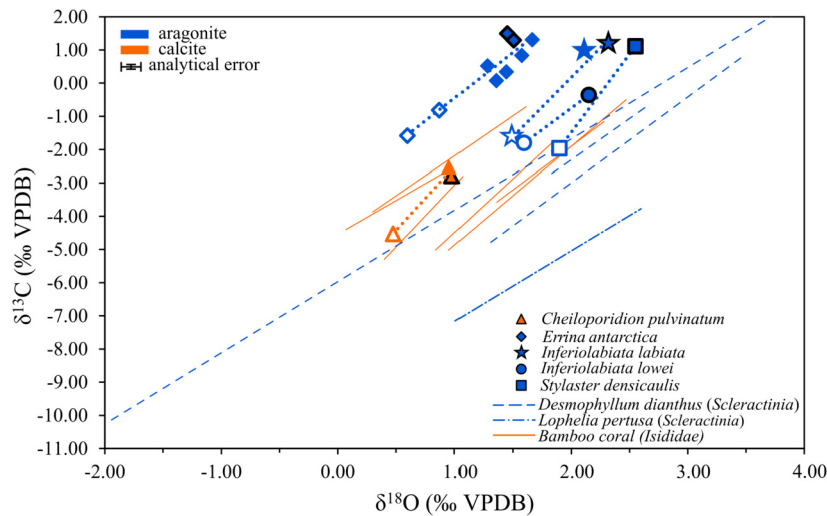**Fig. 4. $\delta^{13}C$ v. $\delta^{18}O$ data for different parts of the coral skeleton within single specimens with least-squares regression lines for each coral.** Least squares regression analyses were performed for each individual stylasterid coral, with slopes ranging from 2.6 to 4.7. Shown as symbols are the stylasterid specimens of this study. Symbols outlined in black are main trunk samples, symbols filled in colour without outline are secondary branch samples and empty symbols outlined in colour are tip samples. Shown as lines are scleractinian and bamboo corals data from Adkins et al. (2003) and Hill et al. (2011). Each line represents the best linear fit for the data within single specimens, and it is not extrapolated past the maximum and minimum $\delta^{18}O$ measured in the specimen. Error bars represent analytical error.
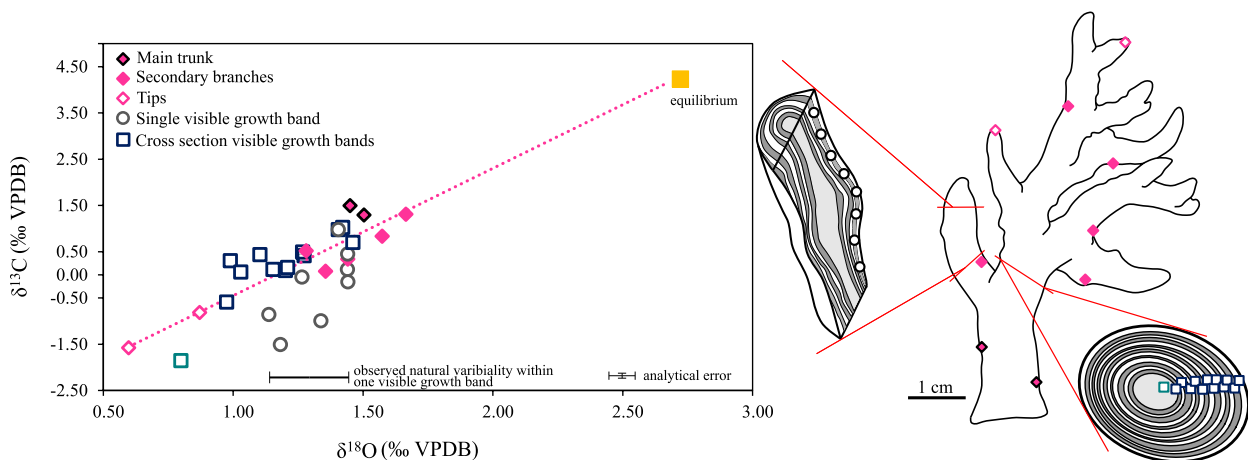

Fig. 5. $\delta^{13}C$ v. $\delta^{18}O$ data of a single specimen of *Errina antarctica*, and sketch of the colony and where each sample was obtained. Pink line is the least-squares regression line for main trunk, secondary branch and tip samples. Orange square represents isotopic equilibrium for aragonite estimated from Grossman and Ku (1986) and Romanek et al. (1992).

+0.28‰ for $\delta^{18}O$ and from −8.09 to −5.13‰ for $\delta^{13}C$ (Table 3). A student's t-test ($\alpha = 0.05$) indicates that the $\delta^{18}O$ and $\delta^{13}C$ depletion values of calcitic and aragonitic samples are statistically different (*p*-value < 0.001).

Fractionation from isotope equilibrium was similar for most of the genera for both $\delta^{18}O$ and $\delta^{13}C$. ANOVA tests ($\alpha = 0.05$) indicate, however, that the mean $\delta^{18}O$ offset value of *Cheiloporidion sp.* and *Conopora sp.* are statistically different from *Stylaster spp.* (*p*-

value < 0.01) and that the mean δ^{13}C offset value of *Conopora sp.* is statistically different from those of *Inferiolabiata spp.* and *Stylaster spp.* (p-value < 0.001).

4. Discussion

4.1. Isotope fractionation in stylasterid corals

The isotopic fractionation within stylasterid skeletons is not spatially homogeneous, with the growing tips and the central core of the coral being lower than the main trunk samples by up to 1‰ and 3‰ for δ^{18}O and δ^{13}C, respectively (Figs. 4 and 5). The slope in the δ^{13}C:δ^{18}O relationships is similar to those observed in scleractinians and bamboo corals (Fig. 4; Weber and Woodhead, 1972b; Smith et al., 2000, 2002; Adkins et al., 2003; Hill et al., 2011). Scleractinian and bamboo corals belong to the class Anthozoa, whilst stylasterids are Hydrozoa, so this broad similarity in slope points towards some commonality in the "vital effects" occurring in these three distinct taxa of the Phylum Cnidaria.

Despite the observed similarities in the "vital effects" signal, the process through which corals produce their carbonate skeletons and manipulate the isotopic composition of seawater is yet to be fully understood. Whether this process is common across all the coral taxa, or whether there are different pathways to coral biomineralisation also remains unclear. McConnaughey (1989) proposed a biomineralisation model in which the "vital effects" in azooxanthellate scleractinians, and the observed strong correlation in their skeletal δ^{18}O and δ^{13}C, was caused by a kinetic fractionation during the skeletal calcification. Subsequently, Adkins et al. (2003) discovered that the densest areas (Centres of Calcification, COC, thought to be associated with rapid mineralisation) in the scleractinian *Desmophyllum dianthus* do not follow the δ^{18}O:δ^{13}C trend observed in the rest of the skeletal components; the COCs being more depleted in δ^{18}O compared to δ^{13}C. This observation led to a second model of biomineralisation, whereby the isotopic composition is affected by the pH of the extracellular calcifying pool from which the coral precipitates. More recently a fully kinetic model of biomineralisation has been proposed by Chen et al. (2018) in which the enzyme carbonic anhydrase modulates the carbonate chemistry of the calcifying fluid controlling the slope of the δ^{18}O:δ^{13}C relationship. This model suggests that the kinetic mechanism proposed by McConnaughey (1989) dominates the δ^{18}O signature, while the Adkins et al. (2003) mechanism explains most of the range in δ^{13}C and the COC 'kink' observed as scleractinian deep-sea corals reach a minimum δ^{13}C value (~ -8‰) at maximum cell derived CO_2. The presence of the enzyme carbonic anhydrase has not been studied in stylasterids, hence the interpretation of the proposed biomineralisation processes in stylasterids requires further investigation.

In our data, we also find evidence of non-systematic internal isotopic variability within stylasterid growth bands. Although there are some similarities in the "vital effects" shown by the different coral taxa, stylasterids show a much smaller range in δ^{18}O and δ^{13}C than scleractinian and bamboo corals (Fig. 4 and 5; Smith et al., 2000, 2002; Adkins et al., 2003; McConnaughey, 2003; Hill et al., 2011).

In summary, the internal variation in the isotopic composition of different parts of the stylasterid coral skeleton reveal both similarities and differences in biomineralisation between stylasterids (Hydrozoa) and scleractinian and bamboo corals (Anthozoa). However, the narrower ranges in the δ^{18}O data from stylasterid corals in comparison with these other deep-sea coral families raise the potential of δ^{18}O in stylasterid corals as a possible paleoclimate proxy.

4.2. Inter coral isotope variability

Given the internal isotope heterogeneity seen in the growth in tips and trunks careful sampling is required to minimise isotopic overprinting by "vital effects". Therefore, samples from only the main branch of all 95 specimens were examined to explore environmental controls (Fig. 3a and 3b).

4.2.1. Calcitic and aragonitic stylasterid corals
Calcitic stylasterid corals all show a lower δ^{18}O and δ^{13}C signature than the aragonitic colonies collected at the same location (Fig. 3a). Indeed, this result is highlighted by colonies of *Cheiloporidion pulvinatum* with different mineralogy which show statistically different values. This observation, as expected, shows that the skeletal mineralogy of stylasterid corals has an important control of the isotopic signal of the sample in line with the data from aragonite scleractinians compared to calcitic bamboo corals (e.g. Smith et al., 2000; Hill et al., 2011).

4.2.2. Stylasterid genera
Our data indicate that coral calcification in stylasterids occurs in disequilibrium with seawater, showing a mean fractionation of -1.16‰ for aragonitic specimens, with *Adelopora sp.* and *Inferiolabiata spp.* having statistically the same mean fractionation to *Errina spp.* and *Stylaster spp.* Weber and Woodhead (1972a) reported that shallow water specimens of *Distichopora* (39 specimens) and *Stylaster* (6 specimens) precipitated in isotopic equilibrium with seawater for δ^{18}O across a temperature range of ~ 5 °C. However, we recalculated the fractionation of these samples considering δ^{18}O of seawater at each location (Schmidt et al., 1999) and the δ^{18}O:temperature calibration determined by Grossman and Ku (1986). The re-evaluated data reveals a mean fractionation of -0.5‰ for *Distichopora* and of -0.6‰ for *Stylaster*. This fractionation is consistent with the range of -0.2 to -1.65‰ that we observed for deep-sea *Stylaster spp.* More recently, Wisshak et al. (2009) recorded that *Errina dabneyi* (growing at ~ 12 °C in the Azores) had a mean negative offset of -0.9‰, similar to the -1.2‰ we observed for *Errina spp.*

Although the existing data does not allow us to rule out genus or species-specific differences in fractionation, we focus the remainder of the discussion on assessing the potential of a "universal" aragonitic stylasterid temperature calibration.

4.3. Stylasterid δ^{18}O temperature proxy

Our results provide evidence that the δ^{18}O of stylasterid corals is temperature dependent and unlocks the possibility of their use as paleotemperature proxies.

To assess the potential of δ^{18}O as a paleotemperature proxy in aragonitic stylasterid corals, we present a universal calibration that could provide a predictive relationship for seawater temperature based on the δ^{18}O stylasterid values. While the specimens analysed for this calibration are geographically constrained to the Atlantic Ocean and eastern Pacific, the diversity of genera included in the calibration suggests that this calibration is likely to be valid for aragonitic stylasterid corals globally. The least squares regression analysis for all the aragonitic samples in this study (77 main trunk samples and 20 bulk samples) yields the following equation:

$$\delta^{18}O_{\text{coral-seawater}} = -0.27(\pm 0.01) \times T(^{\circ}C) + 3.46(\pm 0.06)$$

$$(R^2 = 0.82; \ p\text{-value} < 0.0001) \tag{1}$$

For the mean δ^{18}O value (2.58‰), 95% prediction intervals produced a temperature uncertainty of ± 3.5 °C (95% confidence intervals $= \pm 0.3$ °C).
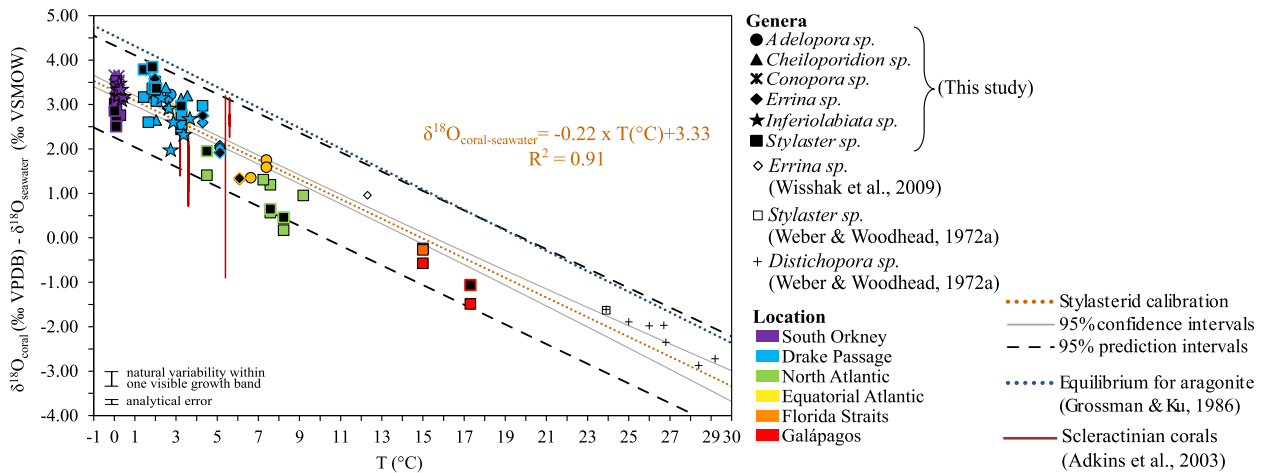
Fig. 6. δ^{18}**Ocoral-seawater v. T (°C) calibration for aragonitic stylasterid corals** of this study and stylasterid samples from Weber and Woodhead (1972a) and Wisshak et al. (2009). Least-squares regression line of the calibration (orange dotted line), 95% prediction intervals (grey dashed line), and 95% confidence intervals (grey continuous line) are included. Symbols and colours represent genera and location, respectively. Colour-filled symbols are main trunk samples of this study. Black-filled symbols outlined in colour are bulk samples of this study. Empty symbols outlined in black are data modified from Weber and Woodhead (1972a) and Wisshak et al. (2009). Each red vertical bar represents δ^{18}O variability measured in a single specimen of scleractinian coral (Adkins et al., 2003). The blue dotted line represents the calibration for aragonite precipitating in isotopic equilibrium with seawater from Grossman and Ku (1986).

This stylasterid δ^{18}O:temperature relationship has a similar slope to the biogenic aragonite in equilibrium calibration (Grossman and Ku, 1986), with an average offset of $\sim$1.2‰. The only other deep-sea stylasterid δ^{18}O data (*Errina dabneyi*), from the Azores, is consistent with this temperature relationship (Wisshak et al., 2009).

When extended to include data from shallow-water stylasterids, the δ^{18}O:temperature relationship is remarkably similar (Weber and Woodhead, 1972a). The data do indicate that there is a smaller fractionation in these shallow water samples, which may be species-specific effects in warm water hydrozoans or analytical artifacts. The δ^{18}O:temperature relationship was recalculated for the samples of this study and those available in the literature (Weber and Woodhead, 1972a; Wisshak et al., 2009) yielding the following equation (Fig. 6):

$$\delta^{18}O_{coral-seawater} = -0.22(\pm0.01) \times T(°C) + 3.33(\pm0.06)$$

$$(R^2 = 0.91; p\text{-value} < 0.0001) \tag{2}$$

In this calibration (Eq. (2)), for the mean δ^{18}O value (2.21‰), 95% prediction intervals produced a temperature uncertainty of ±4.4°C (95% confidence intervals = ±0.5°C).

The data suggest that there could be differences in isotopic fractionation between genera. To test this, we considered each separate genus using least squares regression analyses (Fig. S1 and Table S3). The temperature estimation uncertainty for each of the genera are larger than those given for all genera combined, and in some cases the temperature range is only of $\sim$2 to 4°C. Following these limitations, the universal calibration is preferred at this time (Eq. (2)).

4.4. Potential for time-series analyses

The temperature dependence of δ^{18}O in stylasterid corals, paired with the growth bands observed in skeletal cross-sections, raises the possibility of their use as high-resolution archives of the recent or distant past (e.g. King et al., 2018). A better understanding of biomineralisation processes, growth rates and micro-skeletal structure in stylasterids could aid in the acquisition of a more accurate paleotemperature calibration for this purpose.

Few previous studies have looked at the growth rates and lifespan of stylasterid corals. Imaging and geochemical measurements

have produced differing growth rate estimates, but whether this is due to method accuracy or species/site-specific differences is unknown (Miller et al., 2004; Wisshak et al., 2009; King et al., 2018). In-situ photographic observations of *Errina dabneyi* recorded a linear extension of 4 to 6 mm/yr in the branch length (Wisshak et al., 2009). Calcein staining and imaging methods for the shallow-water *Errina novaezelandiae* suggested an average linear extension of 7 mm/yr in the colony width but growth was found to be highly variable (Miller et al., 2004). Finally, King et al. (2018) found a maximum growth rate of 0.5 mm/yr in length extension using radiocarbon dating methods on *Errina sp*. These growth rates give estimated ages of 70 to 100 yr for *Errina dabneyi* ($\sim$40 cm high), 30 to 40 yr for *Errina novaezelandiae* (20 to 30 cm in diameter), and $\sim$ 200 to 400 yr for *Errina sp*. (9 to 20 cm high).

We find similarities between the internal variability of δ^{18}O and δ^{13}C from our *Errina antarctica* sub-sampled across growth bands (Fig. 5) and that of Wisshak et al. (2009) across a section of *Errina dabneyi*. *Errina antarctica* yield a δ^{18}O range of 0.66‰ and a δ^{13}C range of 0.91‰, while *Errina dabneyi* produce a δ^{18}O range of 0.74‰ and a δ^{13}C range of 1.37‰. Furthermore, our *Errina antarctica* show isotopic depletion for δ^{18}O and δ^{13}C in the growth bands in or near the central core, which is also reflected in Wisshak et al. (2009) who observed a depletion in δ^{13}C in the central growth band, although no obvious shift in the δ^{18}O (Fig. 7). At face value these ranges in δ^{18}O could translate to temperature changes of 2.4 and 2.7°C in magnitude. This variation in the temperatures recorded by single individuals (at 130 m in the sub-Antarctic and 500 m in the Azores, respectively) residing within the thermocline are not unrealistic. It is not yet clear, however, why the centre of the branches and the growing tips are systematically lower in δ^{18}O and δ^{13}C compared to the rest of the skeleton and whether this represents a different biomineralisation processes. It might be that the initial calcification and growing tips calcify rapidly, and posterior thickening of the branches occurs at a slower pace, diminishing kinetic fractionation of δ^{18}O (Adkins et al., 2003). In any case, additional studies focusing on detailed internal variability within stylasterid corals are needed to understand these mechanisms in order to fully exploit these corals as paleoclimate archives.

Another consideration to be made prior to using stylasterids as paleotemperature archives is to understand potential post-mortem diagenesis. Wisshak et al. (2009) observed the presence of secondary carbonate precipitation infilling the canals of the coral
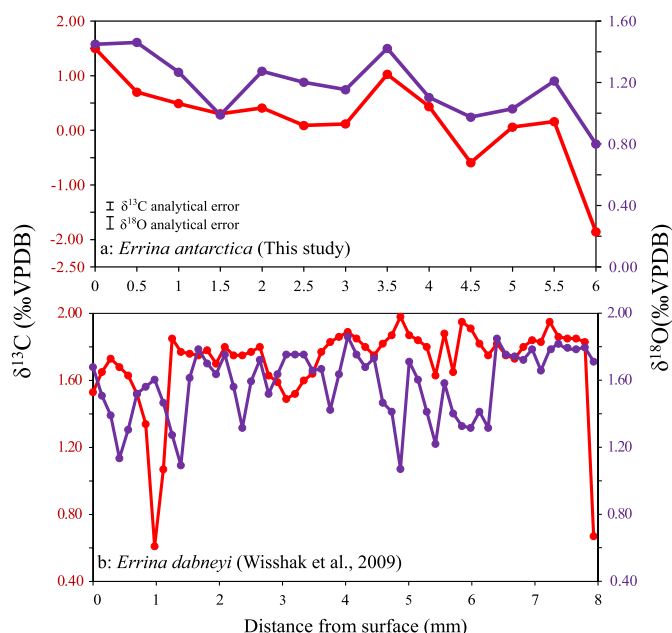
Fig. 7. δ^{13}C and δ^{18}O **data from a cross-section.** (a) Data from a cross-section on *Errina antarctica* plotted against the distance from the surface of the colony. Each datapoint corresponds to a visible growth band in the cross-section. (b) δ^{13}C and δ^{18}O data from a cross-section on *Errina dabneyi* (Wisshak et al., 2009).

skeleton in *Errina dabneyi* and, although its origins (biotic or abiotic) remained unresolved, the bulk isotope composition of this specimen fits within our overall temperature calibration. Likewise, a study comparing living and sub-fossil samples of *Stylaster erubescens* found a significant variability in the presence and degree of taphonomic and diagenetic alteration among these samples, but, encouragingly, δ^{18}O and δ^{13}C data appeared consistent (Black and Andrus, 2012). Therefore, we suggest that aragonitic stylasterid corals represent practical substrates for paleoceanographic temperature reconstruction providing care is exercised in sample selection. Our work shows that, whereas there is risk of inaccurate temperature reconstruction when using highly calcitic specimens, the benefits of developing a temperature proxy that is available from many depths and many locations within the oceans will play an important role in understanding the spatial and temporal pattern of heat absorption into the interior ocean.

5. Conclusions

We propose stylasterid corals as a new high-resolution archive of intermediate and deep-water temperature as recorded in the oxygen isotope composition of their skeletons. They present a degree of internal variability of up to $\sim$0.8‰ and $\sim$4‰ for δ^{18}O and δ^{13}C, respectively. A major finding of this study is that stylasterids present limited internal variability in both δ^{13}C and δ^{18}O when compared to other deep-sea corals. The tips of the skeleton are always lower than the main trunk or branches for both δ^{18}O and δ^{13}C and further studies focusing on growth aspects of these corals may elucidate isotope fractionation effects and best sampling practices for time series work. The δ^{13}C:δ^{18}O linear relationships within individual specimens are similar to those reported in previous studies for deep-sea scleractinian and bamboo corals, and suggest that the isotope composition of stylasterid corals contains "vital effects" similar to other coral groups.

The difference observed in how the δ^{18}O and δ^{13}C relate within different parts of a single coral indicate that different biomineralisation processes act as the corals grow. We encourage future studies to be directed towards the better understanding of biomin-

eralisation mechanisms, the micro-skeletal structure, the δ^{18}O and δ^{13}C composition, and diagenetic alteration in different genera of stylasterid corals.

We find skeletal mineralogy affects the δ^{18}O and δ^{13}C composition of stylasterids, with calcitic specimens showing lower δ^{18}O and δ^{13}C than aragonitic specimens when compared to calculated equilibrium values. For this reason, only aragonitic samples are considered for a temperature calibration.

We present a universal δ^{18}O:temperature calibration for aragonitic stylasterids and temperatures ranging from 0 to 30 °C. This demonstrates that temperature is recorded in the skeletal chemistry of stylasterid corals, thus suggesting the use of stylasterid δ^{18}O records to produce high spatial and temporal resolution timeseries of past seawater temperature. This similar temperature dependency is robust across the seven aragonitic genera tested here. We recommend future research to further confirm this behaviour across the diverse Stylasteridae family (30 extant genera, Cairns, 2011).

To further explore the potential of stylasterids as temperature proxies, different dating techniques should be tested on these taxa aiming for the obtainment of growth rates, lifespan and age of the specimen. Current methods used for dating corals (U-series, radiocarbon and ^{210}Pb) each present limitations and advantages and will have to be implemented on stylasterid corals as well to obtain accurate chronologies. Future work directed towards new proxy development in stylasterid corals, specifically trace metals and clumped isotopes, are highly welcomed in order to unravel the multi-proxy utility of this promising taxon.

Declaration of competing interest

The authors declare that they have no known competing financial interests or personal relationships that could have appeared to influence the work reported in this paper.

Appendix A. Supplementary material

Supplementary material related to this article can be found online at https://doi.org/10.1016/j.epsl.2020.116407.

References

Adkins, J.F., Boyle, E.A., Curry, W.B., Lutringer, A., 2003. Stable isotopes in deep-sea corals and a new mechanism for "vital effects". Geochim. Cosmochim. Acta 67, 1129–1143. https://doi.org/10.1016/S0016-7037(00)01203-6.

Alpert, A.E., Cohen, A.L., Oppo, D.W., DeCarlo, T.M., Gove, J.M., Young, C.W., 2016. Comparison of equatorial Pacific sea surface temperature variability and trends with Sr/Ca records from multiple corals. Paleoceanography 31, 252–265. https://doi.org/10.1002/2015pa002897.

Beck, J.W., Edwards, R.L., Ito, E., Taylor, F.W., Recy, J., Rougerie, F., Joannot, P., Henin, C., 1992. Sea-surface temperature from coral skeletal strontium/calcium ratios. Science 257, 644–647. https://doi.org/10.1126/science.257.5070.644.

Black, H., Andrus, C.F.T., 2012. Taphonomy and diagenesis on the deep-sea hydrocoral Stylaster erubescens fossils from the Charleston Bump. Univ. Alabama McNair J. 12, 19–40.

Cairns, S.D., 2011. Global diversity of the Stylasteridae (Cnidaria: Hydrozoa: Athecatae). PLoS ONE 6. https://doi.org/10.1371/journal.pone.0021670.

Cairns, S.D., 2007. Deep-water corals: an overview with special reference to diversity and distribution of deep-water scleractinian corals. Bull. Mar. Sci. 81, 311–322.

Cairns, S.D., 1992. Worldwide distribution of the Stylasteridae (Cnidaria: Hydrozoa). Sci. Mar. 56, 125–130.

Cairns, S.D., 1991a. A generic revision of the Stylasteridae (Coelenterata: Hydrozoa). Part 3. Keys to the genera. Bull. Mar. Sci. 49, 538–545.

Cairns, S.D., 1991b. The marine fauna of New Zealand: Stylasteridae (Cnidaria: Hydroida). N.Z. Oceanogr. Inst. Mem. 180.

Cairns, S.D., 1986a. Stylasteridae (Hydrozoa: Hydroida) of the Galapagos Islands. Smithson. Contrib. Zool., 1–42. https://doi.org/10.5479/si.00810282.426.

Cairns, S.D., 1986b. A revision of the Northwest Atlantic Stylasteridae (Coelenterata: Hydrozoa). Smithson. Contrib. Zool., 1–131. https://doi.org/10.5479/si.00810282.418.

Cairns, S.D., 1983. Antarctic and Subantarctic Stylasterina (Coelenterata: Hydrozoa). Antarct. Res. Ser. 38, 61–164. https://doi.org/10.1029/AR038p0061.

Cairns, S.D., Macintyre, I.G., 1992. Phylogenetic implications of calcium carbonate. https://doi.org/10.2307/3514799.

Case, D.H., Robinson, L.F., Auro, M.E., Gagnon, A.C., 2010. Environmental and biological controls on Mg and Li in deep-sea scleractinian corals. Earth Planet. Sci. Lett. 300, 215–225. https://doi.org/10.1016/j.epsl.2010.09.029.

Chen, S., Gagnon, A.C., Adkins, J.F., 2018. Carbonic anhydrase, coral calcification and a new model of stable isotope vital effects. Geochim. Cosmochim. Acta 236, 179–197. https://doi.org/10.1016/j.gca.2018.02.032.

Cheng, L., Abraham, J., Hausfather, Z., Trenberth, K.E., 2019. How fast are the oceans warming? Science 363, 128–129. https://doi.org/10.1126/science.aav7619.

Craig, H., 1957. Isotopic standards for carbon and oxygen and correction factors for mass-spectrometric analysis of carbon dioxide. Geochim. Cosmochim. Acta 12, 133–149. https://doi.org/10.1016/0016-7037(57)90024-8.

Davis, B.L., Johnson, L.R., Mebrahtu, T., 1986. X-ray quantitative analysis of coal by the reference intensity method. Powder Diffr. 1, 244–255. https://doi.org/10.1017/S0885715600011787.

Dickinson, S.R., McGrath, K.M., 2001. Quantitative determination of binary and tertiary calcium carbonate mixtures using powder X-ray diffraction. Analyst 126, 1118–1121. https://doi.org/10.1039/b103004n.

Emiliani, C., 1955. Pleistocene temperatures. J. Geol. 63, 538–578. https://doi.org/10.1086/626295.

Emiliani, C., Hudson, J.H., Shinn, E.A., George, R.Y., 1978. Oxygen and carbon isotopic growth record in a reef coral from the Florida Keys and a deep-sea coral from Blake Plateau. Science 202, 627–629. https://doi.org/10.1126/science.202.4368.627.

Epstein, S., Buchsbaum, R., Lowenstam, H.A., Urey, H.C., 1953. Revised carbonate-water isotopic temperature scale. Geol. Soc. Am. Bull. 64, 1315–1325. https://doi.org/10.1130/0016-7606(1953)64.

Fowell, S.E., Sandford, K., Stewart, J.A., Castillo, K.D., Ries, J.B., Foster, G.L., 2016. Intrareef variations in Li/Mg and Sr/Ca sea surface temperature proxies in the Caribbean reef-building coral Siderastrea siderea. Paleoceanography 31, 1315–1329. https://doi.org/10.1002/2016PA002968.

Ghosh, P., Adkins, J., Affek, H., Balta, B., Guo, W., Schauble, E.A., Schrag, D., Eiler, J.M., 2006. ^{13}C-^{18}O bonds in carbonate minerals: a new kind of paleothermometer. Geochim. Cosmochim. Acta 70, 1439–1456. https://doi.org/10.1016/j.gca.2005.11.014.

Gleckler, P.J., Durack, P.J., Stouffer, R.J., Johnson, G.C., Forest, C.E., 2016. Industrial-era global ocean heat uptake doubles in recent decades. Nat. Clim. Change 6, 394–398. https://doi.org/10.1038/nclimate2915.

Grossman, E.L., Ku, T.L., 1986. Oxygen and carbon isotope fractionation in biogenic aragonite: temperature effects. Chem. Geol. Isot. Geosci. Sect. 59, 59–74. https://doi.org/10.1016/0168-9622(86)90057-6.

Heikoop, J.M., Dunn, J.J., Risk, M.J., Schwarcz, H.P., McConnaughey, T.A., Sandeman, I.M., 2000. Separation of kinetic and metabolic isotope effects in carbon-13 records preserved in reef coral skeletons. Geochim. Cosmochim. Acta 64, 975–987. https://doi.org/10.1016/S0016-7037(99)00363-4.

Hendry, K.R., Huvenne, V.A.I., Robinson, L.F., Annett, A., Badger, M., Jacobel, A.W., Ng, H.C., Opher, J., Pickering, R.A., Taylor, M.L., Bates, S.L., Cooper, A., Cushman, G.G., Goodwin, C., Hoy, S., Rowland, G., Samperiz, A., Williams, J.A., Achterberg, E.P., Arrowsmith, C., Alexander Brearley, J., Henley, S.F., Krause, J.W., Leng, M.J., Li, T., McManus, J.F., Meredith, M.P., Perkins, R., Woodward, E.M.S., 2019. The biogeochemical impact of glacial meltwater from Southwest Greenland. Prog. Oceanogr. 176, 102126. https://doi.org/10.1016/j.pocean.2019.102126.

Hill, T.M., Spero, H.J., Guilderson, T., Lavigne, M., Clague, D., MacAlello, S., Jang, N., 2011. Temperature and vital effect controls on bamboo coral (Isididae) isotope geochemistry: a test of the "lines method". Geochem. Geophys. Geosyst. 12. https://doi.org/10.1029/2010GC003443.

Hughes, T.P., Kerry, J.T., Álvarez-Noriega, M.G., Álvarez-Romero, J., Anderson, K.D., Baird, A.H., Wilson, S.K., 2017. Global warming and recurrent mass bleaching of corals. Nature 543, 373–377. https://doi.org/10.1038/nature21707.

King, T.M., Rosenheim, B.E., Post, A.L., Gabris, T., Burt, T., Domack, E.W., 2018. Large-scale intrusion of Circumpolar Deep Water on Antarctic margin recorded by stylasterid corals. Paleoceanogr. Paleoclimatol. 33, 1306–1321. https://doi.org/10.1029/2018PA003439.

Lauvset, S.K., Key, R.M., Olsen, A., Van Heuven, S., Velo, A., Lin, X., Schirnick, C., Kozyr, A., Tanhua, T., Hoppema, M., Jutterström, S., Steinfeldt, R., Jeansson, E., Ishii, M., Perez, F.F., Suzuki, T., Watelet, S., 2016. A new global interior ocean mapped climatology: the 1° × 1° GLODAP version 2. Earth Syst. Sci. Data 8, 325–340. https://doi.org/10.5194/essd-8-325-2016.

Lea, D.W., 2014. Elemental and isotopic proxies of past ocean temperatures. In: Treatise on Geochemistry, 2nd ed. Elsevier, Oxford.

Lindner, A., Cairns, S.D., Cunningham, C.W., 2008. From offshore to onshore: multiple origins of shallow-water corals from deep-sea ancestors. PLoS ONE 3. https://doi.org/10.1371/journal.pone.0002429.

Marcott, S.A., Clark, P.U., Padman, L., Klinkhammer, G.P., Springer, S.R., Liu, Z., Otto-Bliesner, B.L., Carlson, A.E., Ungerer, A., Padman, J., He, F., Cheng, J., Schmittner, A., 2011. Ice-shelf collapse from subsurface warming as a trigger for Heinrich events. Proc. Natl. Acad. Sci. 108, 13415–13419. https://doi.org/10.1073/pnas.1104772108.

Martínez-Botí, M.A., Foster, G.L., Chalk, T.B., Rohling, E.J., Sexton, P.F., Lunt, D.J., Pancost, R.D., Badger, M.P.S., Schmidt, D.N., 2015. Plio-Pleistocene climate sensitivity evaluated using high-resolution CO$_2$ records. Nature 518, 49–54. https://doi.org/10.1038/nature14145.

McConnaughey, T., 1989. ^{13}C and ^{18}O isotopic disequilibrium in biological carbonates: I patterns. Geochim. Cosmochim. Acta 53, 151–162. https://doi.org/10.1016/0016-7037(89)90282-2.

McConnaughey, T.A., 2003. Sub-equilibrium oxygen-18 and carbon-13 levels in biological carbonates: carbonate and kinetic models. Coral Reefs 22, 316–327. https://doi.org/10.1007/s00338-003-0325-2.

McCrea, J.M., 1950. On the isotopic chemistry of carbonates and a paleotemperature scale. J. Chem. Phys. 18, 849–857. https://doi.org/10.1063/1.1747785.

Miller, K.J., Mundy, C.N., Chadderton, W.L., 2004. Ecological and genetic evidence of the vulnerability of shallow-water populations of the stylasterid hydro coral Errina novaezelandiae in New Zealand's fiords. Aquat. Conserv. Mar. Freshw. Ecosyst. 14, 75–94. https://doi.org/10.1002/aqc.597.

Montagna, P., McCulloch, M., Douville, E., López Correa, M., Trotter, J., Rodolfo-Metalpa, R., Dissard, D., Ferrier-Pagès, C., Frank, N., Freiwald, A., Goldstein, S., Mazzoli, C., Reynaud, S., Rüggeberg, A., Russo, S., Taviani, M., 2014. Li/Mg systematics in scleractinian corals: calibration of the thermometer. Geochim. Cosmochim. Acta 132, 288–310. https://doi.org/10.1016/j.gca.2014.02.005.

O'Neil, J.R., Clayton, R.N., Mayeda, T.K., 1969. Oxygen isotope fractionation in divalent metal carbonates. J. Chem. Phys. 51, 5547–5558. https://doi.org/10.1063/1.1671982.

Roberts, J.M., Wheeler, A.J., Freiwald, A., 2006. Reefs of the deep: the biology and geology of cold-water coral ecosystems. Science 312, 543–547. https://doi.org/10.1126/science.1119861.

Robinson, L.F., Adkins, J.F., Frank, N., Gagnon, A.C., Prouty, N.G., Brendan Roark, E., de van Flierdt, T., 2014. The geochemistry of deep-sea coral skeletons: a review of vital effects and applications for palaeoceanography. Deep-Sea Res., Part 2, Top. Stud. Oceanogr. 99, 184–198. https://doi.org/10.1016/j.dsr2.2013.06.005.

Romanek, C.S., Grossman, E.L., Morse, J.W., 1992. Carbon isotopic fractionation in synthetic aragonite and calcite: effects of temperature and precipitation rate. Geochim. Cosmochim. Acta 56, 419–430. https://doi.org/10.1016/0016-7037(92)90142-6.

Schmidt, G.A., Bigg, G.R., Rohling, E.J., 1999. Global seawater oxygen-18 database - v1.22 [WWW document]. https://data.giss.nasa.gov/o18data/.

Smith, J.E., Schwarcz, H.P., Risk, M.J., 2002. Patterns of isotopic disequilibria in azooxanthellate coral skeletons. Hydrobiologia 471, 111–115. https://doi.org/10.1023/A:1016553304276.

Smith, Jodie E., Schwarcz, H.P., Risk, M.J., McConnaughey, T.A., Keller, N., 2000. Paleotemperatures from deep-sea corals: overcoming "vital effects". Palaios 15, 25. https://doi.org/10.2307/3515589.

Smith, S.V., Buddemeier, R.W., Redalje, R.C., Houck, J.E., 1979. Strontium-calcium thermometry in coral skeletons. Science 204, 404–407. https://doi.org/10.1126/science.204.4391.404.

Spooner, P.T., Guo, W., Robinson, L.F., Thiagarajan, N., Hendry, K.R., Rosenheim, B.E., Leng, M.J., 2016. Clumped isotope composition of cold-water corals: a role for vital effects? Geochim. Cosmochim. Acta 179, 123–141. https://doi.org/10.1016/j.gca.2016.01.023.

Thiagarajan, N., Adkins, J., Eiler, J., 2011. Carbonate clumped isotope thermometry of deep-sea corals and implications for vital effects. Geochim. Cosmochim. Acta 75, 4416–4425. https://doi.org/10.1016/j.gca.2011.05.004.

Urey, H.C., 1947. The thermodynamic properties of isotopic substances. J. Chem. Soc., 562–581. https://doi.org/10.1039/jr9470000562.

Weber, J.N., Woodhead, P.M.J., 1972a. Temperature dependence of oxygen-18 concentration in reef coral carbonates. J. Geophys. Res. 77, 463–473. https://doi.org/10.1029/JC077i003p00463.

Weber, J.N., Woodhead, P.M.J., 1972b. Stable isotope ratio variations in nonscleractinian coelenterate carbonates as a function of temperature. Mar. Biol. 15, 293–297. https://doi.org/10.1007/BF00401388.

Wisshak, M., López Correa, M., Zibrowius, H., Jakobsen, J., Freiwald, A., 2009. Skeletal reorganisation affects geochemical signals, exemplified in the stylasterid hydrocoral *Errina dabneyi* (Azores Archipelago). Mar. Ecol. Prog. Ser. 397, 197–208. https://doi.org/10.3354/meps08165.

Zibrowius, H., Cairns, S.D., 1992. Revision of the Northeast Atlantic and Mediterranean Stylasteridae (Cnidaria: Hydrozoa). Mem. Museum Natl. d'Histoire Natl. Ser. A Zool. 153, 1–136.